GEODYNAMICS & TECTONOPHYSICS
Published by the Institute of the Earth's Crust, Siberian Branch, Russian Academy of Sciences
PALEOGEODYNAMICS

2023 VOLUME 14 ISSUE 4 ARTICLE 0707
ISSN 2078-502X

DOI: 10.5800/GT-2023-14-4-0707

KENGEDE MAFIC DYKE SWARM AND EXPANSION OF THE 1.50 Ga KUONAMKA LARGE IGNEOUS PROVINCE OF NORTHERN SIBERIA

M.D. Tomshin [1], **R.E. Ernst** [2,3], **U. Söderlund** [4], **A.V. Okrugin** [1]✉

[1] Diamond and Precious Metal Geology Institute, Siberian Branch of the Russian Academy of Sciences, 39 Lenin Ave, Yakutsk 677000, Russia
[2] Carleton University, Ottawa K1S 5B6, Ontario, Canada
[3] National Research Tomsk State University, 36 Lenin Ave, Tomsk 634050, Russia
[4] Lund University, Lund 223 62, Sweden

ABSTRACT. Within the Anabar shield in the northern part of the Siberia, Late Precambrian mafic igneous units are widespread, which form dyke swarms of different ages of different trends. This paper presents new data on the composition, structure and U-Pb dating of the E-W trending Kengede dyke swarm. Three new U-Pb ID-TIMS baddeleyite ages (1496±7, 1494±3 and 1494±5 Ma) were obtained from three dykes, indicating that the Kengede swarm is part of the 1500 Ma Kuonamka large igneous province (LIP). The previously recognized Kuonamka Large Igneous Province (LIP) extends for 700 km from the Anabar shield to the Olenek uplift in the northern part of the Siberia and is potentially linked to coeval dykes and sills of the São Francisco craton and the Congo craton. The newly dated Kengede swarm is parallel to but offset by 50 km from the previously dated 1501±3 Ma Kuonamka swarm, and the identification of these two subparallel dyke subswarms of the Kuonamka LIP supports the earlier interpretation that mantle plume centre was located along the extrapolated trend of the dykes near the eastern or western margin of the Siberia. The paper examines features of sulfide Cu-Ni mineralization in dolerites of the Kengede and East Anabar dyke swarms and discusses potential Cu-Ni-sulfide mineralization linked to the Precambrian mafic dyke swarms of different ages in the north-east of the Siberia.

KEYWORD: basite; dike swarm; large igneous province; plume; Anabar shield; Siberian craton

FUNDING: Geological and petrological section of the work was carried out within the framework of the DPMGI SB RAS (0381-2019-0003) and the LIPs-Industry Consortium project (www.supercontinent.org), section on Cu-Ni-sulfide mineralization was carried out within the framework of the Russian Science Foundation project (Regional contest) 22-27-20151.

RESEARCH ARTICLE

Received: November 14, 2022
Revised: March 27, 2023
Accepted: April 11, 2023

Correspondence: Alexander V. Okrugin, okrugin@diamond.ysn.ru

FOR CITATION: Tomshin M.D., Ernst R.E., Söderlund U., Okrugin A.V., 2023. Kengede Mafic Dyke Swarm and Expansion of the 1.50 Ga Kuonamka Large Igneous Province of Northern Siberia. Geodynamics & Tectonophysics 14 (4), 0707. doi:10.5800/GT-2023-14-4-0707

1. INTRODUCTION

The Anabar shield in the north-eastern part of the Siberian craton is host to mafic dykes and sills hosted in Archean–Proterozoic metamorphosed rocks and Riphean age (Fig. 1). Isotope-geochronological data of sedimentary rocks of the western and eastern framing of the Anabar shield [Gorokhov et al., 2019] shows that they belong to the Lower Riphean (1600–1400 Ma). This is confirmed by the maximally young U-Pb age of 1681±28 Ma detritus zircons from the basal horizons of the Mukun sandstones of the eastern margin of the Anabar shield [Khudoley et al., 2015].

Late Precambrian K-Ar ages of mafic dykes were first produced during the medium-scale geological mapping in the 60s [Mashchak, 1969; Oleinikov et al., 1983]. Later, mineralogical and petrochemical studies of these dykes along with further K-Ar dating was undertaken throughout the the Anabar shield and revealed multiple trends of dykes up to 200–300 km and a range of Precambrian ages [Okrugin et al., 1990]. More recently precise U-Pb dating, was produced for three of the swarms and each was interpreted to represent the exposed plumbing system of a LIP:

– NW-trending dykes of the 1385 Ma Chieress [Ernst et al., 2000] and their also extension into the Taimyr [Priyatkina et al., 2018] and Udzha paleo-rift [Malyshev et al., 2018];

– EW-trending dykes (and sills) of the 1500 Ma Kuonamka LIP [Ernst et al., 2000, 2016b];

– NNW-trending dykes of the 1774–1750 Ma Eastern Anabar portion of the Timpton LIP [Gladkochub et al., 2010, 2019, 2022; Ernst et al., 2016a].

This article presents new U-Pb dating of the Kengede dyke swarm (Fig. 2) located subparallel and 50 km to the south of the Kuonamka swarm. The need for these studies is to clarify the age of the Kengede swarm formation in order to compare it with other dyke belts of the Anabar shield.

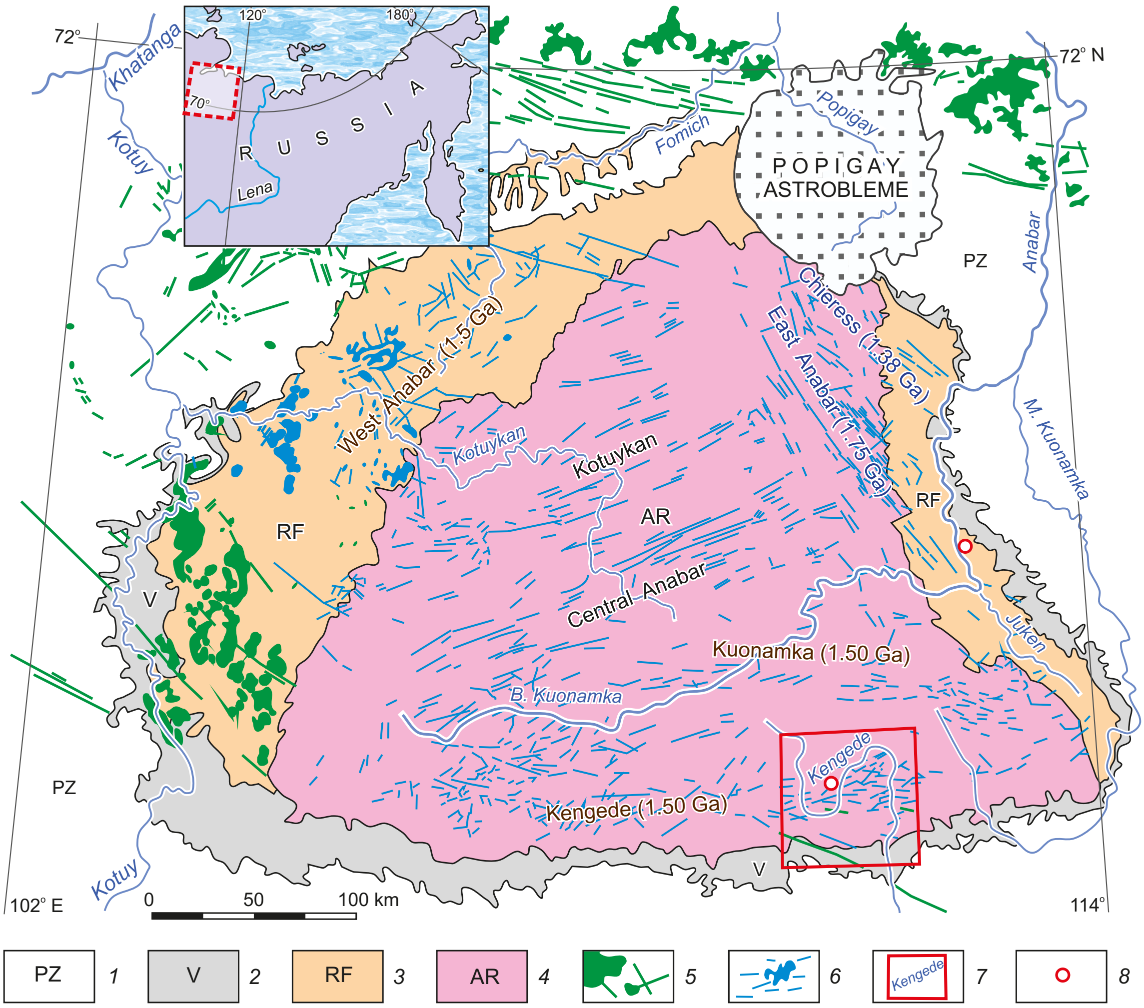

Fig. 1. Scheme of distribution of dyke swarms and sill province in Anabar shield after [Okrugin et al., 1990; Ernst et al., 2016b]. *1* – Paleozoic dolomites, limestones, marlstones and sandstones; *2* – Vendian dolomites,sandstones, argillite, conglomerates and limestones; *3* – Riphean conglomerates, sandstones, siltstones, argillite and dolomites; *4* – Archean-Paleoproterozoic metamorphic complexes; *5* – Permian-Triassic sills and dikes of Siberian trapp; *6* – Late Precambrian dyke swarms with their age (Kuonamka (1.50 Ga) etc.); *7* – the site of the studied dykes of the Kengede swarm (Fig. 2); *8* – location of the dolerite with Cu-Ni sulfide mineralization. Constructed on the basis of a Geological maps of the Anabar Shield, scale 1:1000000 [State Geological Map..., 1983], and Siberian platform, scale 1:1500000 [Geological Map..., 1999] with some changes and additions by the authors.

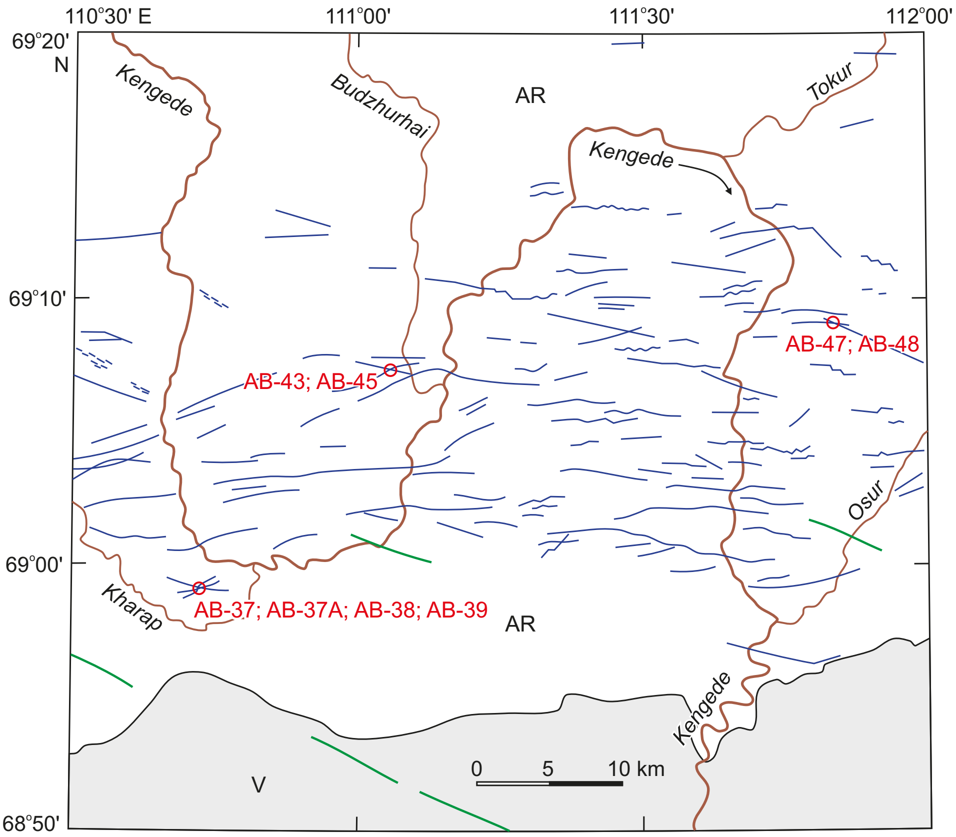

Fig. 2. Fragment of the Kengede dyke swarm in the Kengede River basin (see Fig. 1).
Distrubition of dykes is shown according to the geological map of scale 1:200000 [Geological Map..., 1975], with the location of three groups studied dykes (red circles) and sample numbers (AB-37, etc.).

Ranking of all dike swarms of the Anabar Shield can be useful in carrying out further paleotectonic constructions. In addition, Based on the identification of sulfide Cu-Ni mineralization in the dolerites of the Bujurkhai dyke of the Kengede dyke swarm [Mashchak, 1969] and dolerites of the East Anabar dyke swarm [Okrugin et al., 2021], their potential Cu-Ni mineralization of Late Precambrian basites is discussed in a view of the model proposed in the works of [Jowitt, Ernst, 2013; Ernst, Jowitt, 2013].

2. GEOLOGICAL AND PETROCHEMICAL CHARACTERISTICS OF THE KENGEDE BASITE DYKE SWARM

On the basis of trend the dykes of the Anabar shield can be divided into multiple swarms: sublatitudinal trending Kengede, and Kuonamka, ENE trending Central Anabar, Kotuykan, and West Anabar), NNW trending East Anabar, NW trending Chieress swarm [Okrugin et al., 1990]. Within each swarm, the trends typically align in the direction of the overall direction trend the swarm. However, in the sublatitudinal trending Kuonamka and Kengede swarms, the dykes frequently exhibit en-echelon structure and some variation in trends with predominant strikes of 80–90° and 95–103°. Dikes filling feathering cracks of the ENE and WNW directions are less frequently observed (Fig. 2). Diachronous intersecting dykes are observed occasionally, e.g., the Kharap group of three intersecting dykes (Fig. 3).

The dykes of the Kengede swarm cut metamorphic complexes of the basement, but are covered by Vendian-Lower Paleozoic terrigenous-carbonate strata of the platform cover. Some NW trending dykes belong to the the Permian-Triassic Siberian Trap magmatism. The Precambrian dykes have K-Ar ages of 1600–1300 Ma, indicating Early and Middle Riphean emplacement ages [Mashchak, 1969; Oleinikov et al., 1983; Okrugin et al., 1990]. In order to determine the U-Pb age for the Kengede swarm, three dykes were sampled in the middle course of the Kengede River: AB-(37–39) – dykes of the Kharap stream; AB-(43, 45) – dykes of the Budjurkhai stream; and AB-(47, 48) – dykes from the watershed area of the Kengede-Osur rivers (see Fig. 2).

The sampled dykes are unmetamorphosed and fresh in appearance. They are characterized by sharp cross-cutting contacts and a steep dip. In the endocontact zone (near margin portion), the dykes are composed of microdolerite that transitions into more coarse-graded gabbro-dolerites in the dyke interior. The thickness of the rocks mainly ranges from a few meters to the first tens of meters and less often reaches 100–200 m. The dykes can be traced in length from several tens of meters to several kilometers, depending on their thickness.

The Kengede dykes are medium-grained ophitic gabbro-dolerites consisting of plagioclase, augite, olivine, titanomagnetite, quartz-feldspar mesostasis and minor amphibole and micaceous minerals. Dykes with the greatest thickness have a complex interior structure due to the differentiation of the melt. Such dyke transition from quartz gabbro-dolerites in the marginal zones to gabbro-diorites and monzonite-porphyries in the central part. For example, in the Kharap dykes, the central zone with a thickness of 12–16 m is composed of quartz monzonite porphyries that have distinct boundaries with host mafic units (Fig. 3). Numerous aplitic veins with a thickness of up to 3 cm are also observed in this dyke [Mashchak, 1970].

Geochemistry of the studied Kengede dykes is compared with that of the Kuonamka swarm are shown in Table 1. The Table 1 also provides weighted mean values for the Precambrian mafic dykes of the Kengede swarm, which are divided into tholeiitic and subalkalic rock series according to their petrochemical characteristics [Oleinikov et al., 1983]. In the SiO_2–(Na_2O+K_2O) diagram, samples selected for isotopic dating are confined mainly to the field of basalts of subalkalic composition, while dolerites most enriched in SiO_2 dyke AB-37 of the Kharap stream group dykes (Fig. 3) gravitate to the field of basaltic andesites (Fig. 4, a). However, dykes from the Bujurkhai stream area are characterized by increased alkalis at a relatively low SiO_2 content and, similarly to subalkalic dolerites, approach the field of trachybasalts. Dykes of the Kengede swarm are compositionally similar to those of the Kuonamka swarm [Ernst et al., 2016b] and generally fall within the range of Precambrian mafic units of the Anabar shield. A wider range of Anabar mafic units related to the development of basaltic trachyandesites and trachyandesites is due to the occurrence of late differentiates in complex dykes, represented by quartz monzonite-porphyries.

According to the other geochemical parameters, dolerites of the Kengede swarm are also identical to the Kuonamka dykes. Among the latter, two geochemical groups were identified [Ernst et al., 2016b]. These two groupings are particularly clear shows in the Ti-V diagram (Fig. 4, b) where Group 1 plot within the OFB-CFB-MORB field, while Group 2 plot mostly in the OIB-ALK field. Compared to the rocks of the first group, those of the second group are more enriched with titanium, potassium, phosphorus and REE. Unfortunately, only a small number of trace element analyses are available for Kengede dyke swarm. However, these limited geochemical data also fully correspond to those of the Kuonamka dykes. In the Zr-Ti-Y discriminant diagram

Table 1. Chemical composition (wt. %) and content of trace elements (ppm) in the rocks of the Kengede dyke swarm

Dyke	Kharap				Budjurkhai		Osur		Kengede swarm		Kuonamka swarm	
Samle	AB-37	AB-37A	AB-38	AB-39	AB-43	BD*	AB-47	AB-48	T-B*	SAB*	94-04*	94-03*
SiO_2	51.52	49.36	49.65	48.89	47.57	47.42	48.39	49.07	51.84	49.17	52.96	49.97
TiO_2	2.99	1.81	2.56	2.02	2.55	3.60	2.23	2.08	2.45	3.51	1.75	3.09
Al_2O_3	14.12	13.75	12.71	13.00	12.09	12.22	12.9	12.79	13.77	12.70	12.75	13.60
Fe_2O_3	3.80	1.25	3.89	3.54	6.98	5.67	3.52	5.57	4.67	5.54	14.35//	13.62//
FeO	10.75	11.91	11.45	12.12	10.65	11.07	10.81	9.96	8.99	9.48	–	–
MnO	0.12	0.19	0.20	0.21	0.23	0.14	0.24	0.22	0.19	0.17	0.22	0.21
MgO	3.83	7.40	5.88	6.27	6.10	5.87	7.60	6.06	4.93	5.29	5.35	5.83
CaO	7.51	9.76	9.28	9.93	9.37	8.90	10.02	9.99	7.73	7.55	9.71	9.48
Na_2O	2.61	2.82	2.34	2.05	2.18	2.70	1.99	2.10	2.88	3.33	2.29	2.67
K_2O	1.30	0.34	0.61	0.42	0.47	0.62	0.63	0.75	1.36	1.17	0.45	0.92
P_2O_5	0.40	0.17	0.28	0.22	0.20	0.26	0.26	0.19	0.31	0.48	0.17	0.62
LOI	1.40	0.81	1.63	1.75	2.30	1.38	1.66	1.65	0.95	1.60	1.24	1.52
n	1	1	1	1	1	25	1	1	33	40	1	1
Total	100.35	99.57	100.48	100.42	100.69	99.85	100.25	100.43	100.07	99.97	101.24	101.53
Ni	53	100	–	–	–	82	–	–	78	59	62	89
Co	33	37	–	–	–	43	–	–	37	36	51	42
Cr	26	92	–	–	–	95	–	–	68	53	40	90
V	253	429	–	–	–	505	–	–	345	373	427	332
Sc	28	40	–	–	–	49	–	–	36	36	37	25
Zn	–	107	–	–	–	63	–	–	55	32	123	161
Cu	253	337	–	–	–	260	–	–	208	154	189	84
Pb	2.5	4	–	–	–	2.4	–	–	4.0	3.3	2	7

Note. * – previously published data: BD – weighted mean values of the Budjurkhai dyke group (n=25); T-B and SAB – compositions of the tholeiite-basalt (n=33) and subalkaline basalt (n=40) respectively of the Kengede swarm dykes by [Oleinikov et al., 1983]; 94-04 and 94-03 correspond to EG94-04-05 (Group 1) and EG94-03-05 (Group 2) of the Kuonamka swarm by [Ernst et al., 2016b], where // – total Fe_2O_3+FeO. The remaining data relate to the newly dated dykes of the Kengede swarm. Silicate analyses were carried out by wet chemistry, and trace elements were determined by spectral analysis in laboratories of the DPMGI SB RAS. n – number of analysis.

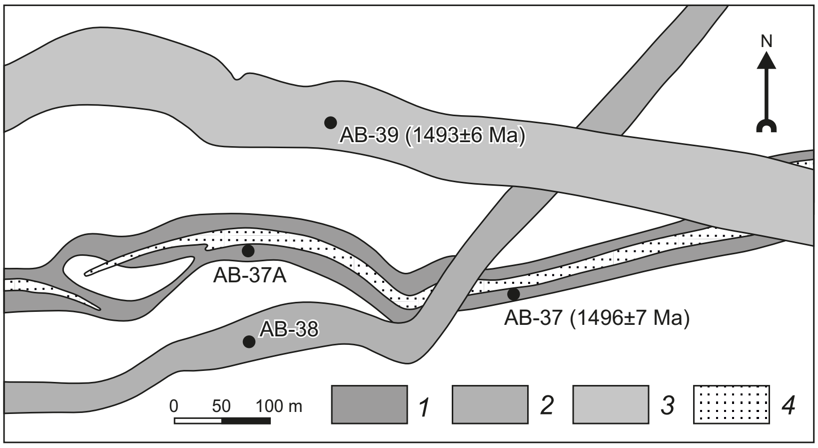

Fig. 3. Field site map locating the three crosscutting dykes of the Kharap stream group of dykes after [Mashchak, 1970]. *1–3* – gabbro-dolerite of the dykes AB-37, AB-38 and AB-39, respectively with U-Pb age; *4* – monzonite-porphyry.

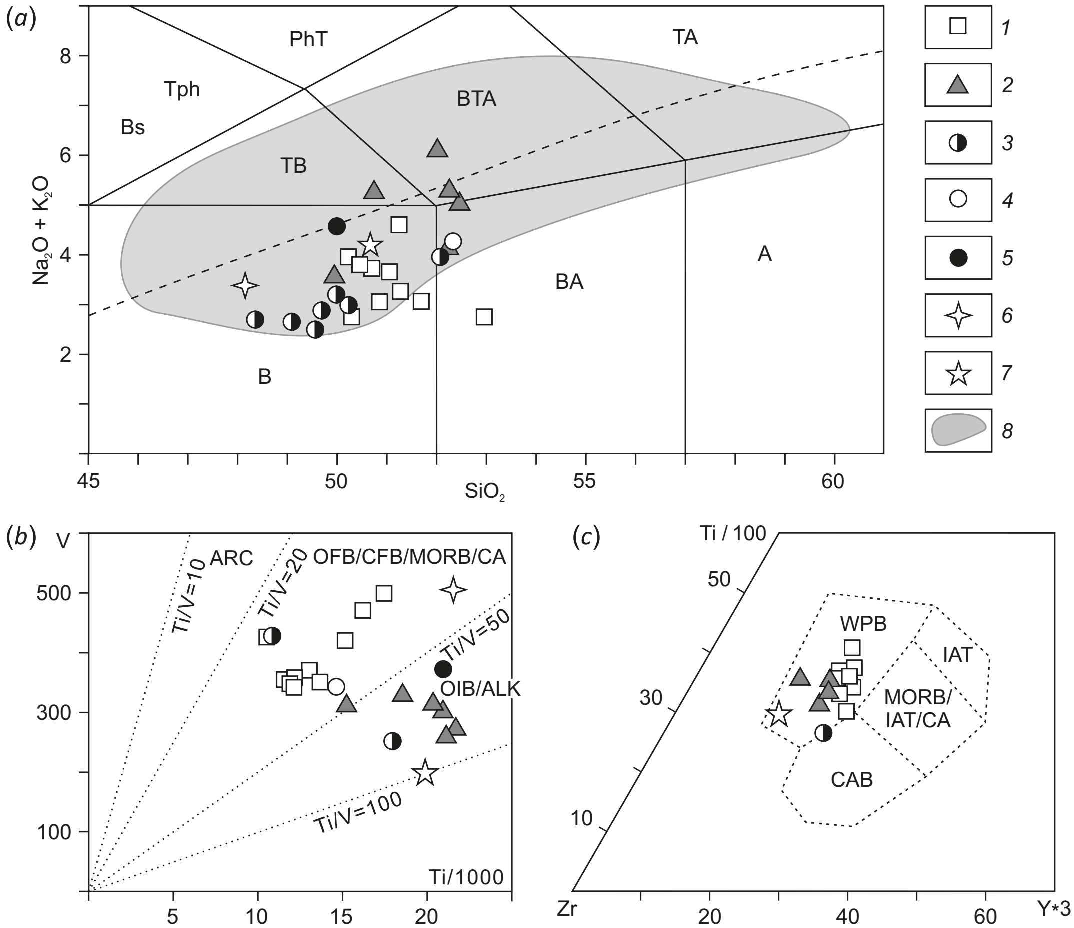

Fig. 4. Compositions of the Kuonamka LIP units on geochemical diagrams.
(*a*) – SiO_2–(Na_2O+K_2O) diagram based on the systematics of the International Union of Geological Sciences (IUGS, 2002): B – basalt; BA – basaltic andesite; A – andesite; TA – trachyandesite; BTA – basaltic trachyandesite; TB – trachybasalt; Bs – basanite; Tph – tephrite; PhT – phonotephrite. Dotted line shows the boundary between alkaline (above the line) and subalkaline rocks. Rock compositions are calculated for dry residual; (*b*) – V-Ti diagram [Shervais, 1982], ARC – arc tholeiites, OFB – oceanic flood basalt, CFB – continental flood basalt, MORB – mid-ocean-ridge basalt, CA – calc-alkaline basalt, OIB – oceanic island basalts, ALK – alkali basalt; (*c*) – Zr-Ti-Y discriminant diagram [Pearce, Cann, 1973], WPB – within-plate basalts, IAT – island-arc tholeiites, CAB – calc-alkaline basalts. *1–2* – basites of the first (*1*) and second (*2*) groups of the Kuonamka LIP [Ernst et al., 2016b]; *3* – dykes of the Kengede river studied by the authors (Table 1); *4–6* – weighted mean values of the Kenegede swarm dykes of the tholeiite-basalt (*4*) and subalkaline (*5*) compositions, and Budjurkhai dykes (*6*) [Oleinikov et al., 1983]; *7* – dolerites with sulfide nodules, Bolshaya Kuonamka river [Okrugin et al., 2021]; *8* – field of compositions of the Late Precambrian basites of the Anabar shield [Mashchak, 1970; Oleinikov et al., 1983; Okrugin et al., 1990; Koroleva et al., 1999].

(Fig. 4, c), the Kengede swarm, as well as the Kuonamka swarm, plot in the field of intraplate basalts.

3. U-Pb GEOCHRONOLOGY OF THE KENGEDE DYKE SWARM AND INTERPRETATION

Three dikes of the Kengede swarm were dated by the U-Pb ID-TIMS (isotope dilution-thermal ionisation mass spectrometry) method. These samples were processed at the University of Lund laboratory using the baddeleyite separation method [Söderlund, Johansson, 2002]. Approximately 30 brown baddeleyite grains were separated from each sample, except sample AB37 from which only 6 grains were obtained. Baddeleyite grains are of good quality and the optically best grains were handpicked and combined into four fractions for sample AB-39 and AB-45, and two fractions for sample AB-37. Two-to four grains were combined in each fraction. Isotopic analysis was performed on a Finnigan TRITON mass spectrometer at the Natural History of Museum in Stockholm. All fractions were analyzed in peak-switching mode using the SEM (Secondary Electron Multiplier). The U-Pb data are presented in Table 2 and Fig. 5 and discussed below:

AB-37: Two fractions were prepared but one failed. The successful fraction plots ca. 1 % discordant yielding a Pb^{207}/Pb^{206} age of 1496±7 Ma (Fig. 5, a, dark grey ellipse).

AB-39: All 4 fractions overlap and plot less than 1 % discordant (Fig. 5, a, light grey ellipses). Including all the fractions in the age calculation yields a weighted Pb^{207}/Pb^{206}

Table 2. U-Pb TIMS data for baddeleyte from the Kengede dolerites

Analysis no.	Number of grains	U/Th	Pb_c/Pb_{tot} 1)	$^{206}Pb/^{204}Pb$ 2)	Isotope ratios 3)				Age, Ma						Concordance
					$^{207}Pb/^{235}U$	±2σ	$^{206}Pb/^{238}U$	±2σ	$^{207}Pb/^{235}U$	±2σ	$^{206}Pb/^{238}U$	±2σ	$^{207}Pb/^{206}U$	±2σ	
Sample AB-39															
Bd-1	3	14.6	0.045	1485.8	3.3087	0.71	0.25731	0.66	1483.1	5.5	1476.1	8.7	1493.2	5.4	0.989
Bd-2	5	22.6	0.115	532.1	3.3083	0.72	0.25834	0.67	1483.0	5.6	1481.4	8.9	1485.4	5.7	0.997
Bd-3	4	17.0	0.069	946.2	3.3235	0.81	0.25818	0.78	1486.6	6.3	1480.5	10.3	1495.2	5.6	0.990
Bd-4	4	n.m.	0.037	1772.5	3.3403	0.46	0.25964	0.43	1490.5	3.6	1488.0	5.7	1494.2	3.7	0.996
Sample AB-37															
Bd-1	2	13.6	0.071	928.6	3.3411	0.89	0.25945	0.85	1490.7	7.0	1487.0	11.2	1496	6.6	0.994
Sample AB-45															
Bd-5	2	17.3	0.028	2415.8	3.3234	0.46	0.25873	0.43	1486.6	3.6	1483.4	5.7	1491.1	3.6	0.995
Bd-6	2	16.3	0.051	1253.9	3.3346	0.55	0.25937	0.47	1489.2	4.3	1486.6	6.2	1492.8	5.5	0.996
Bd-7	3	2.7	0.295	157.7	3.3605	0.67	0.26008	0.45	1495.2	5.3	1490.3	6.0	1502.3	8.9	0.992
Bd-8	4	39.3	0.032	2081.2	3.3391	0.44	0.25935	0.40	1490.2	3.4	1486.5	5.3	1495.5	3.8	0.994

Note. Bd – baddeleyite. 1) Pb_c – common Pb; Pb_{tot} – total Pb (radiogenic + blank + initial). 2) Measured $^{206}Pb/^{204}Pb$ ratio, corrected for fractionation and spike. 3) Isotopic ratios corrected for fractionation (0.1 % per amu for Pb), spike contribution, blank (0.5 pg Pb and 0.05 pg U), and initial common Pb. Initial common Pb corrected with isotopic compositons from the model of [Stacey, Kramers, 1975] at the age of the sample. n.m. – not measured.

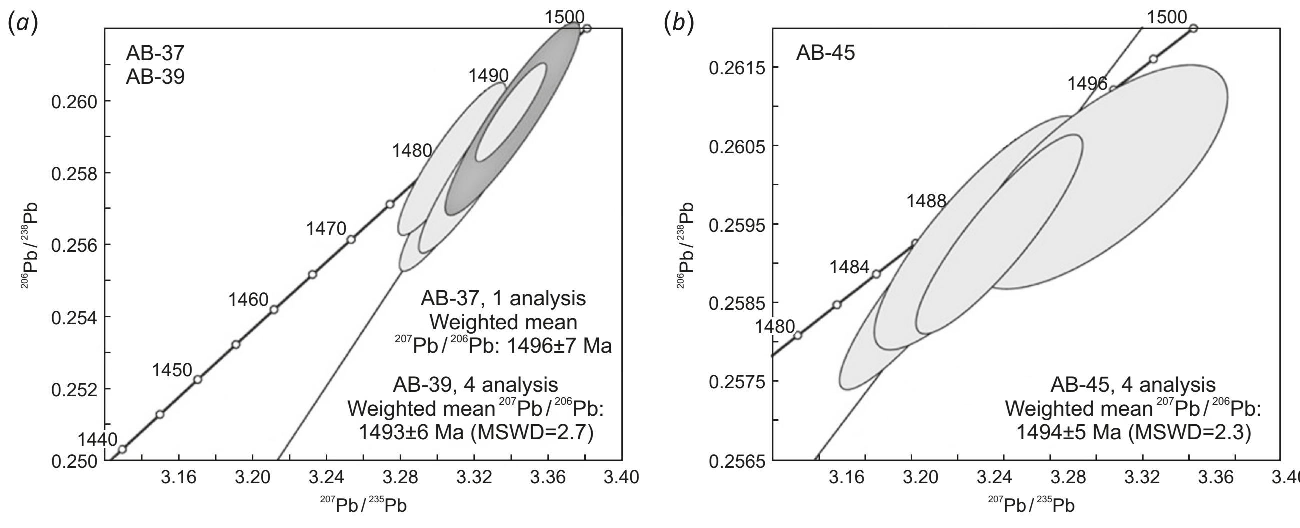

Fig. 5. Concordia diagrams showing U–Pb baddeleyite ID-TIMS results. (*a*) – data for samples AB-37 (dark grey) and AB-39 (light-grey); (*b*) – for sample AB-45. Dashed lines represent regressions anchored at 0 Ma.

mean age of 1493±6 Ma. Excluding the least radiogenic fraction, that plots slightly off, results in a weighted mean of 1494±3 Ma.

AB-45: For this sample the 4 fractions overlap and plot concordant within uncertainty (Fig. 5, b). The weighted mean of $Pb^{207}/^{206}$ dates is 1494±5 Ma, and this is the preferred age of this dyke.

Therefore, it can be summarized that the obtained new baddeleyite ages (1496±7; 1494±3 and 1494±5 Ma) of the three dykes from the E-W trending Kengede swarm match the age (1501–1503 Ma) of the EQ94-04-05 dolerite dyke, located along the Bolshaya Kuonamka River [Ernst et al., 2016b]. Fig. 6 provides a summary of the available 11 U-Pb ages currently available for the Kuonamka LIP (8 in [Ernst et al., 2016b], and 3 U-Pb ages produced herein). The 10 U-Pb ID-TIMS ages show ages between 1505 and 1495 Ma.

Thus, the correspondence of the time of formation and mineralogical and geochemical features of the dykes of the Kengede belt with the dykes of the adjacent Kuonamka swarm allows us to consider them as interconnected and parallel sub-swarms belonging to the Kuonamka LIP. One of the main unanswered questions for the Kuonamka LIP is the location of the plume centre. That two adjacent sub-swarms separated by a dyke-poor gap (Kuonamka and now the Kengede) have similar E-W trends provides additional support for these dykes providing evidence for the location of the plume centre, likely located along the eastern or western extension of the Kuonamka and Kengede sub-swarms to (or beyond) the eastern or western edge of the

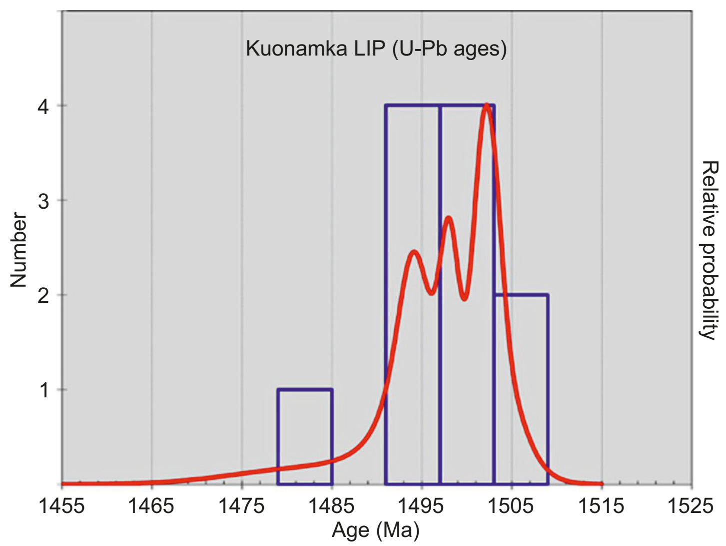

Fig. 6. Cumulative U-Pb age spectrum for the Kuonamka LIP. Plot produced using Isoplot 4.15 [Ludwig, 2012].

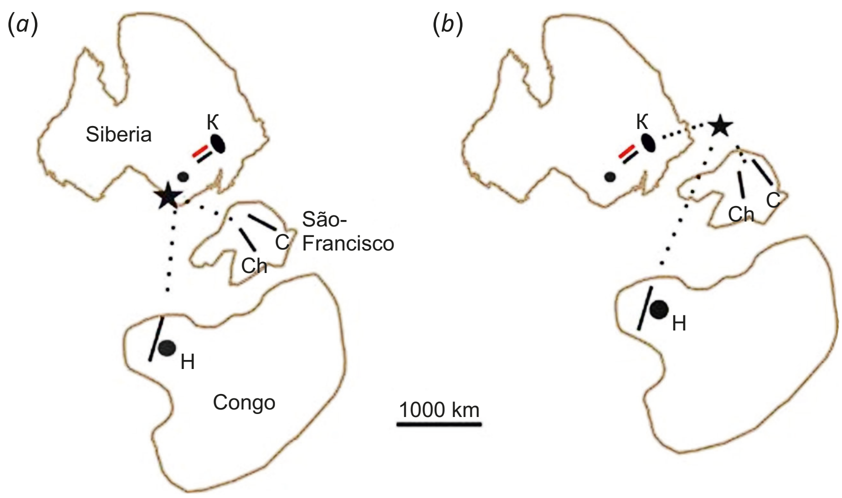

Fig. 7. 1500 Ma magmatism superimposed on two alternative reconstruction of northern Siberia with the combined São Francisco-Congo craton after [Ernst et al., 2016b].
(*a*) – modified from [Ernst et al., 2013] with the interpreted plume located east of the Siberian craton; (*б*) – modified from [Cederberg et al., 2016] with the interpreted plume located to the west of the Siberian craton. K = Kuonamka LIP consisting of Western Anabar sills (black oval), Kuonamka subswarm (black line), Olenek sills (small circle) and Kengede subswarm (red line), the latter identified herein; C, Curaçá; Ch, Chapada Diamantina dykes of the Sao Francisco craton; H, Humpata sills and dykes of the Congo craton.

Siberian craton. The greatly expanded scale of the 1501 Ma Kuonamka LIP extends for 700 km in northern Siberia (from the Anabar Shield to the Olenek uplift), can be correlated temporarily with dyke and sill province in the formerly attached São Francisco and Congo craton (Fig. 7), and is consistent with available paleomagnetic data [Ernst et al., 2013]. This results in a single, short duration, high-volume LIP event that is over 2000 km across, and therefore represents a particularly large LIP event [Ernst et al., 2016b].

4. LINK OF KENGEDE AND KUONAMKA SUBSWARMS TO SOURCE MAFIC-ULTRAMAFIC INTRUSIONS WITH PGE-CU-NI ORE DSPOSITS

Mafic-ultramafic intrusions of LIPs are highly prospective for PGE-Cu-Ni deposits [Naldrett, 2010; Ernst, Jowitt, 2013; Smith, Maier, 2021; etc.]. It is well-established that large sulfide PGE-Cu-Ni deposits are mostly associated with Precambrian basic-ultrabasic rocks, i.e. the Canadian shield (Sudbury, Thompson), Baltic shield (Monchegorsk, etc.), Australian shield (Kambalda), and others. The Proterozoic platinum-bearing massifs of southern Siberia associated with LIP are considered by [Mekhonoshin et al., 2016]. In general, the Phanerozoic lacks the occurrences of sulfide-bearing magmatic formations, with the exception of the Norilsk deposits that are the largest among such deposits [Genkin et al., 1981; Distler et al., 1988; Likhachev, 2006; Smith, Maier, 2021].

By comparison with the 1270 Ma Mackenzie dyke swarm of Canada [Baragar et al., 1996; Blanchard et al., 2017], the presence of two narrow subswarms of dykes separated by a dyke-poor region (50 km wide) may indicate lateral emplacement of the subswarms from different layered intrusions located at the end of the subswarms (Fig. 8). Analysis of such subswarms for chalcophile content can potentially be a useful strategy for assessing ore potential in the potential source magmatic chambers [Jowitt, Ernst, 2013; Ernst, Jowitt, 2013]. If chalcophile element depletion is observed in one (or both) of these subswarms (S1 or S2, in Fig. 8), then the corresponding layered intrusion (M-UM-1 or M-UM-2) may be enriched in such chalcophile elements, and thus may have ore potential. In this particular case, such chalcophile element data are not available for the Kuonamka dykes and the hypothesized M-UM (mafic-ultramafic layered intrusions) and plume centre location remain to be determined. The radius of the plume centre region is estimated at several hundred km up to about 500 km and the location of the S1 and S2 subswarms could be at least many hundreds of km away from the plume centre region.

S1 and S2 are subswarms 1 and 2 (analogous to the Kuonamka and Kengede subswarms of this study). M-UM-1 and -2 are layered intrusions near the plume centre that are hypothesized to be feeding the subswarms. In this case the plume centre is shown located to the east, but in the case of the Kuonamka LIP a plume centre to the west remains possible. Some examples of copper-nickel sulfide ore occurrences in the dolerites of the Kengede and East-Anabar dyke swarms are studied in relation to such a model of the formation of potentially ore-bearing magmatites. They have a very limited value and small size, and the location of the plume center is not known, so we cannot predict possible locations of layered intrusions with large ore content.

Within the Kengede swarm, areas with disseminated and stringer-disseminated sulfide copper-nickel mineralization have been established in the dykes in the Kharap and Budjurkhai stream areas [Mashchak, 1969; Oleinikov et al., 1983]. These areas are confined to taxitic-textured dolerites and can be traced for hundreds of meters, with a width of 2–6 m, reaching 8-9 m in local swells. The outlines of the mineralized zones are indistinct, with sulfide content usually being 1–5 %, less often reaching 10–15 %. The size of sulfide grains ranges from less than 1 mm to 5–10 mm. The outlines of small grains are of irregular angular shape, due to their interstitial nature. Composition of the phenocrysts is homogeneous and includes pyrrhotite (90–95 %) and chalcopyrite. Large schlieren bodies of sulfides have an irregular, less often isometric shape with

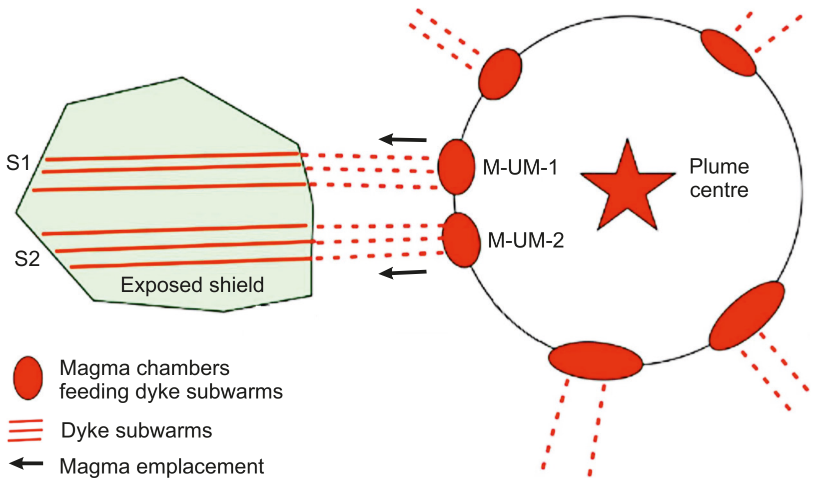

Fig. 8. Lateral feeding of subswarms (S1and S2) from a ring of mafic-ultramafic intrusions (M-UM-1,2) in the plume centre region, model after [Baragar et al., 1996; Blanchard et al., 2017; Ernst et al., 2019].

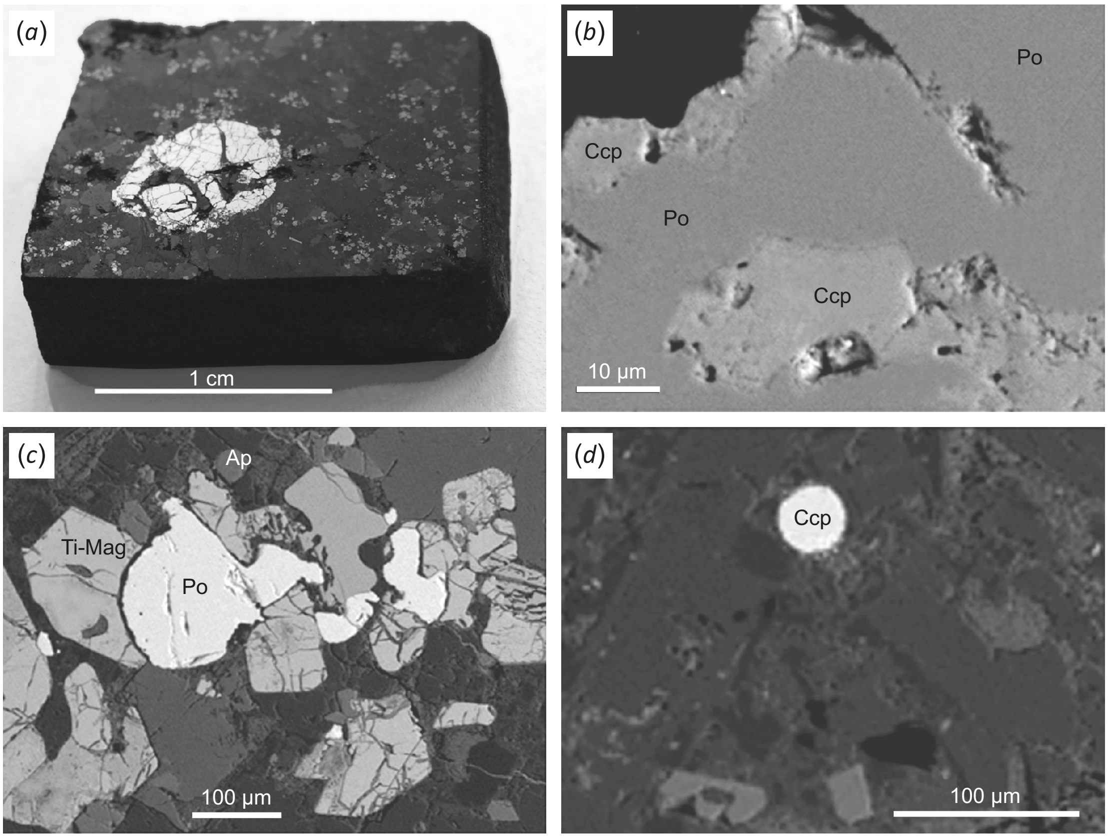

Fig. 9. Minerals of the sulfide nodule in the dolerites (sample L-1388) of the Bol'shaya Kuonamka River.
(*a*) – photo image of the polished sample; (*b*) – intergrowths of chalcopyrite (Ccp) and pyrrhotite (Po); (*c*) – segregation paragenesis of the apatite (Ap), titanomagnetite (Ti-Mag) and pyrrhotite; (*d*) – a drop-like inclusion of chalcopyrite. (*b, c*) – backscatter electron images.

a size of 15–60 mm. Major minerals of the schlieren are titanomagnetite, cubanite, chalcopyrite, and pyrrhotite; minor minerals include pentlandite, makinovite, violarite, valleriite, bravoite, millerite, bornite, and pyrite.

In addition, on the eastern slope of the Anabar shield, on the terrace of the Bolshaya Kuonamka River 18 km below the mouth of the Juken tributary of the B. Kuonamka River (see Fig. 1) in the block of dolerites from a landslides (sample L-1388), visually detectable rounded sulfide nodules ranging in size from 1 to 10 mm across were found (Fig. 9, a) [Okrugin et al., 2021]. The major minerals in sulfide nodules are pyrrhotite and chalcopyrite that form symplectic intergrowths (Fig. 9, b). Clusters of faceted crystals or fused titanomagnetite, which are associated with pyrrhotite and apatite, are frequently formed around the nodule (Fig. 9, c). Apart from the large rounded nodules, small isolated droplets of chalcopyrite and pyrrhotite are also observed in the dolerites, ranging in size from the first microns to 0.1–0.2 mm (Fig. 9, d). The remaining rare sulfide and sulfoarsenide minerals are represented by siegenite, gersdorffite, galena, sphalerite and other phases.

The L-1388 dolerite that host these sulfide phenocrysts are represented by medium-grained light-gray rocks of the ophitic structure. They are composed mainly of plagioclase, clinopyroxene and titanomagnetite; less often they include potassium feldspar, amphibole, orthopyroxene, apatite chlorite, zeolite, quartz, calcite and ilmenite. The L-1388 dolerite belongs to the East Anabar swarm, but the chemistry is similar both those of the Kuonamka and Kengede subswarms (see Fig. 4).

Thus, it can be concluded that the mineral composition of sulfide nodules of the L-1388 dolerites is similar to the stringer-disseminated copper-nickel occurrences from the dykes of the Kengede swarm. Similar associations and morphology of the rare sulfides are typical for the platinum-copper-nickel ores of the Norilsk deposits, as well as the copper-nickel mineralization of the liquid immiscibility type associated with the differentiated Precambrian complexes of mafic-ultramafic rocks of other regions. Overall, this suggests the possible presence of Precambrian mafic units with PGE-Cu-Ni sulfide mineralization in the Anabar shield [Okrugin et al., 2021]. Rounded bodies of sulfide nodules indicate that they are of an early magmatic nature resulted from the silicate-sulfide liquid immiscibility. Under favorable conditions of differentiation of large volumes of such liquates, sulfide ores rich in PGE-Cu-Ni can be formed.

5. CONCLUSION

U-Pb ID-TIMS dating (1496±7; 1494±3 and 1494±5 Ma) of three dykes in the previously undated Kengede dyke swarm of the Anabar Shield of the Siberian craton indicates that this swarm is part of the Kuonamka large igneous province (LIP). The previously recognized Kuonamka LIP extends for 700 km from the Anabar shield to the Olenek uplift in the northern part of the Siberia and is potentially linked to coeval dykes and sills of the San Francisco and Congo cratons. The newly dated EW trending Kengede dykes is located is separated from the 1501 Ma Kuonamka dykes by a 50 km wide dyke-poor region. This indicates that the Kuonamka and Kengede dykes are subswarms of the Kuonamka LIP and the gap can be explained by being laterally fed from two separate magma chambers associate with the plume centre region, which is also confirmed by the similarity of the petrochemical features of the dykes. The location of this plume centre could be beyond the east or west ends of the subswarms. The presence of copper-nickel sulfide ore occurrences of limited importance and small size in the dolerites of the Kengede and East Anabar dyke swarms indicates the potential possibility of their link to layered intrusions with PGE-Cu-Ni deposits.

6. ACKNOWLEDGEMENTS

The authors appreciate the efforts of their colleagues who took part in field and laboratory research, and are also grateful to the reviewers A.S. Mekhonoshin and A.K. Khudoley for valuable comments that helped in improvement of the article.

7. CONTRIBUTION OF THE AUTHORS

The authors contributed equally to this article.

8. CONFLICT OF INTERESTS

The authors have no conflicts of interest to declare. All authors have read and agreed to the published version of the manuscript.

9. REFERENCES

Baragar W.R.A., Ernst R.E., Hulbert L., Peterson T., 1996. Longitudinal Petrochemical Variation in the Mackenzie Dyke Swarm, Northwestern Canadian Shield. Journal of Petrology 37 (2), 317–359. https://doi.org/10.1093/petrology/37.2.317.

Blanchard J.A., Ernst R.E., Samson C., 2017. Gravity and Magnetic Modelling of Layered Mafic-Ultramafic Intrusions in Large Igneous Province Plume Centre Regions: Case Studies from the 1.27 Ga Mackenzie, 1.38 Ga Kunene-Kibaran, 0.06 Ga Deccan, and 0.13–0.08 Ga High Arctic Events. Canadian Journal of Earth Sciences 54 (3), 290–310. https://doi.org/10.1139/cjes-2016-0132.

Cederberg J., Söderlund U., Oliveira E.P., Ernst R.E., Pisarevsky S.A., 2016. U-Pb Baddeleyite Dating of the Proterozoic Pará de Minas Dike Swarm in the São Francisco Craton (Brazil) – Implications for Tectonic Correlation with Siberia, Congo and the North China Cratons. GFF 138 (1), 219–240. https://doi.org/10.1080/11035897.2015.1093543.

Distler V.V., Grokhovskaya T.L., Evstigneeva T.L., Sluzenkin S.F., Filimonova A.A., Duizikov O.A., Laputina I.P., 1988. Petrology of Sulfide Magmatic Ore Formation. Nauka, Moscow, 232 p. (in Russian) [Дистлер В.В., Гроховская Т.Л., Евстигнеева Т.Л., Служенкин С.Ф., Филимонова А.А., Дюжиков О.А., Лапутина И.П. Петрология сульфидного магматического рудообразования. М.: Наука, 1988. 232 с.].

Ernst R.E., Buchan K.L., Hamilton M.A., Okrugin A.V., Tomshin M.D., 2000. Integrated Paleomagnetism and U-Pb Geochronology of Mafic Dikes of the Eastern Anabar Shield Region, Siberia: Implications for Mesoproterozoic Paleolatitude of Siberia and Comparison with Laurentia. The Journal of Geology 108 (4), 381–401. https://doi.org/10.1086/314413.

Ernst R.E., Hamilton M.A., Söderlund U., Hanes J.A., Gladkochub D.P., Okrugin A.V., Kolotilina T., Mekhonoshin A.S., Bleeker W., LeCheminant A.N., Buchan K.L., Chamberlain K.R., Didenko A.N., 2016a. Southern Siberia and Northern Laurentia: Neighbours for a Quarter of Earth's History. Nature Geosciences 9, 464–469. https://doi.org/10.1038/NGEO2700.

Ernst R.E., Jowitt S.M., 2013. Large Igneous Provinces (LIPs) and Metallogeny. In: M. Colpron, T. Bissig, B.G. Rusk, J.F.H. Thompson (Eds), Tectonics, Metallogeny, and Discovery: The North American Cordillera and Similar Accretionary Settings. Society of Economic Geologists Special Publication 17, 17–51. https://doi.org/10.5382/SP.17.02.

Ernst R.E., Liikane D.A., Jowitt S.M., Buchan K.L., Blanchard J.A., 2019. A New Plumbing System Framework for Mantle Plume-Related Continental Large Igneous Provinces and Their Mafic-Ultramafic Intrusions. Journal of Volcanology and Geothermal Research 384, 75–84. https://doi.org/10.1016/j.jvolgeores.2019.07.007.

Ernst R.E., Okrugin A.V., Veselovskiy R.V., Kamo S.L., Hamilton M.A., Pavlov V., Söderlund U., Chamberlain K.R., Rogers C., 2016b. The 1501 Ma Kuonamka Large Igneous Province of Northern Siberia: U-Pb Geochronology, Geochemistry, and Links with Coeval Magmatism on Other Crustal Blocks. Russian Geology and Geophysics 57 (5), 653–671. https://doi.org/10.1016/j.rgg.2016.01.015.

Ernst R.E., Pereira E., Hamilton M.A., Pisarevsky S.A., Rodriques J., Tassinari C.C.G., Teixeira W., Van-Dunem V., 2013. Mesoproterozoic Intraplate Magmatic "Barcode" Record of the Angola Portion of the Congo Craton: Newly Dated Magmatic Events at 1500 and 1110 Ma and Implications for Nuna Supercontinent Reconstructions. Precambrian Research 230, 103–118. https://doi.org/10.1016/j.precamres.2013.01.010.

Genkin A.D., Distler V.V., Gladyshev G.D., Filimonova A.A., Evstigneeva T.L., Kovalenker V.A., Laputina I.P., Smirnov A.V., Grohovskaja T.L., 1981. Sulfide Copper-Nickel Ores of the Norilsk Deposits. Nauka, Moscow, 234 p. (in Russian) [Генкин А.Д., Дистлер В.В., Гладышев Г.Д., Филимонова А.А., Евстигнеева Т.Л., Коваленкер В.А., Лапутина И.П., Смирнов А.В., Гроховская Т.Л. Сульфидные медно-никелевые руды норильских месторождений. М.: Наука, 1981. 234 с.].

Geological Map of Siberian Platform and Adjoining Areas, 1999. Scale 1:1500000. VSEGEI Publishing House, Saint Petersburg (in Russian) [Геологическая карта Сибирской платформы и прилегающих территорий. Масштаб 1:1500000. СПб.: ВСЕГЕИ, 1999].

Geological Map of the USSR, 1975. Scale 1:200000. Sheet R-49-XXVII, XXVIII. VSEGEI Publishing House, Leningrad (in Russian) [Геологическая карта СССР. Масштаб 1:200000. Лист R-49-XXVII, XXVIII. Л.: ВСЕГЕИ, 1975].

Gladkochub D.P., Donskaya T.V., Ernst R.E., Söderlund U., Mazukabzov A.M., Shokhonova M.N., 2019. Enlargement of the Area of the Timpton Large Igneous Province (ca. 1.75 Ga) of the Siberian Craton. Geodynamics and Tectonophysics 10 (4), 829–839 (in Russian) [Гладкочуб Д.П., Донская Т.В., Эрнст Р.Е., Седерлунд У., Мазукабзов А.М., Шохонова М.Н. Расширение ареала Тимптонской крупной магматической провинции (~1.75 млрд лет) Сибирского кратона. Геодинамика и тектонофизика. 2019. Т. 10. № 4. С. 829–839]. https://doi.org/10.5800/GT-2019-10-4-0444.

Gladkochub D.P., Donskaya T.V., Pisarevsky S.A., Ernst R.E., Söderlund U., Kotov A.B., Kovach V.P., Okrugin A.V., 2022. 1.79–1.75 Ga Mafic Magmatism of the Siberian Craton and Late Paleoproterozoic Paleogeography. Precambrian Research 370, 106557. https://doi.org/10.1016/j.precamres.2022.106557.

Gladkochub D.P., Pisarevsky S.A., Donskaya T.V., Ernst R.E., Wingate M.T., Söderlund U., Mazukabzov A.M., Sklyarov E.V., Hamilton M.A., Hanes J.A., 2010. Proterozoic Mafic Magmatism in Siberian Craton: An Overview and Implications for Paleocontinental Reconstruction. Precambrian Research 183 (3), 660–668. https://doi.org/10.1016/j.precamres.2010.02.023.

Gorokhov I.M., Kuznetsov A.B., Semikhatov M.A., Vasil'eva I.M., Rizvanova N.G., Lipenkov G.V., Dubinina E.O., 2019. Early Riphean Billyakh Group of the Anabar Uplift, North Siberia: C–O Isotopic Geochemistry and Pb-Pb Age of Dolomites. Stratigraphy and Geological Correlation 27, 514–528. https://doi.org/10.1134/S0869593819050022.

Jowitt S.M., Ernst R.E., 2013. Geochemical Assessment of the Metallogenic Potential of Proterozoic LIPs of Canada. Lithos 174, 291–307. https://doi.org/10.1016/j.lithos.2012.03.026.

Khudoley A., Chamberlain K., Ershova V., Sears J., Prokopiev A., MacLean J., Kazakova G., Malyshev S., Molchanov A., Kullerud K., Toro J., Miller E., Veselovskiy R., Li A., Chipley D., 2015. Proterozoic Supercontinental Restorations: Constraints from Provenance Studies of Mesoproterozoic to Cambrian Clastic Rocks, Eastern Siberian Craton. Precambrian Research 259, 78–94. https://doi.org/10.1016/j.precamres.2014.10.003.

Koroleva O.V., Okrugin A.V., Rikhvanov L.P., 1999. Complex Dykes of the Anabar Massif – Indicators of Riftogenic Processes. In: Geology and Tectonics of Platform and Orogenic Regions of Northeast Asia. Readings Dedicated to the 80th Anniversary of the Birth of Professor K.B. Mokshantsev. Materials of the Meeting. Vol. 2. Yakutian Scientific Center SB RAS, Yakutsk, p. 80–84 (in Russian) [Королева О.В., Округин А.В., Рихванов Л.П. Сложные дайки Анабарского массива – индикаторы рифтогенных процессов // Геология и тектоника платформ и орогенных областей северо-востока Азии. Чтения к 80-летию со дня рождения профессора К.Б. Мокшанцева: Материалы совещания. Якутск: ЯНЦ СО РАН, 1999. Т. 2. С. 80–84].

Likhachev A.P., 2006. Platinum-Nickel-Copper and Platinum Deposits. Aslan, Moscow, 496 p. (in Russian) [Лихачев А.П. Платино-медно-никелевые и платиновые месторождения. М.: Эслан, 2006. 496 с.].

Ludwig K.R., 2012. ISOPLOT 3.75. A Geochronological Toolkit for Microsoft Excel. User's Manual. Berkeley Geochronology Center Special Publication 5, 75 p.

Malyshev S.V., Pasenko A.M., Ivanov A.V., Gladkochub D.P., Savatenkov V.M., Meffre S., Abersteiner A., Kamenetsky V.S., Shcherbakov V.D., 2018. Geodynamic Significance of the Mesoproterozoic Magmatism of the Udzha Paleo-Rift (Northern Siberian Craton) Based on U-Pb Geochronology and Paleomagnetic Data. Minerals 8 (12), 555. https://doi.org/10.3390/min8120555.

Mashchak M.S., 1969. Sulfide Copper-Nickel Ore Occurrences in Proterozoic Diabase Dikes of the Southern Slope of the Anabar Shield. Geology of Ore Deposits 6, 74–78 (in Russian) [Мащак М.С. Сульфидные медно-никелевые рудопроявления в протерозойских дайках диабазов южного склона Анабарского щита // Геология рудных месторождений. 1969. № 6. С. 74–78].

Mashchak M.S., 1970. Trap Magmatism of the Southern Slope of the Anabar Shield. In: A.M. Vilenskiy (Ed.), Geology and Petrology of Intrusive Traps of the Siberian Platform. Nauka, Moscow, p. 34–48 (in Russian) [Мащак М.С. Траповый магматизм южного склона Анабарского щита // Геология и петрология интрузивных траппов Сибирской платформы / Ред. А.М. Виленский. М.: Наука, 1970. С. 34–48].

Mekhonoshin A.S., Ernst R., Söderlund U., Hamilton M.A., Kolotilina T.B., Izokh A.E., Polyakov G.V., Tolstykh N.D., 2016. Relationship of Platinum-bearing Ultramafic-Mafic Intrusions and Large Igneous Provinces (exemplified by the Siberian Craton). Russian Geology and Geophysics 57 (5), 822–833. https://doi.org/10.1016/j.rgg.2015.09.020.

Naldrett A.J., 2010. Secular Variation of Magmatic Sulfide Deposits and Their Source Magmas. Economic Geology 105 (3), 669–688. https://doi.org/10.2113/gsecongeo.105.3.669.

Okrugin A.V., Oleinikov B.V., Savvinov V.T., Tomshin M.D., 1990. Late Precambrian Dyke Swarms of the Anabar Massif, Siberian Platform, USSR. In: A.J. Parker, P.C. Rickwood, D.H. Tucker (Eds), Mafic Dykes and Emplacement Mechanisms. Proceedings of the Second International Dyke Conference (September 12–16, 1990, Adelaide, South Australia). Balkema, Rotterdam, p. 529–533.

Okrugin A.V., Zemnukhov A.L., Zhuravlev A.I., 2021. Copper-Nickel Sulfide Mineral Occurrence in Dolerites of the Eastern Slope of the Anabar Shield. Arctic and Subarctic Natural Resources 26 (4), 16–28 (in Russian) [Округин А.В., Земнухов А.Л., Журавлев А.И. Медно-никелевое сульфидное рудопроявление в долеритах восточного склона Анабарского щита // Природные ресурсы Арктики и Субарктики. 2021. Т. 26. № 4]. С. 16–28. DOI:10.31242/2618-9712-2021-26-4-16-28.

Oleinikov B.V., Mashchak M.S., Kolodeznikov I.I., Kopylova A.G., Savvinov V.T., Tomshin M.D., Tulasynov B.N., 1983. Petrology and Geochemistry of Basites Intrusions of the Siberian Platform. Nauka, Novosibirsk, 208 p. (in Russian) [Олейников Б.В., Мащак М.С., Колодезников И.И., Копылова А.Г., Саввинов В.Т., Томшин М.Д., Туласынов Б.Н. Петрология и геохимия позднедокембрийских интрузивных базитов Сибирской платформы. Новосибирск: Наука, 1983. 207 с.].

Pearce J.A., Cann J.R., 1973. Tectonic Setting of Basic Volcanic Rocks Determined Using Trace Element Analyses. Earth and Planetary Science Letters 19 (2), 290–300. https://doi.org/10.1016/0012-821X(73)90129-5.

Priyatkina N., Collins W.J., Khudoley A., Zastrozhnov D., Ershova V., Chamberlain K., Shatsillo A., Proskurnin V., 2017. The Proterozoic Evolution of Northern Siberian Craton Margin: A Comparison of U-Pb-Hf Signatures from Sedimentary Units of the Taimyr Orogenic Belt and the Siberian Platform. International Geology Review 59 (13), 1632–1656. https://doi.org/10.1080/00206814.2017.1289341.

Shervais J.W., 1982. Ti-V Plots and the Petrogenesis of Modern and Ophiolitic Lavas. Earth and Planetary Science Letters 59 (1), 101–118. https://doi.org/10.1016/0012-821X(82)90120-0.

Smith W.D., Maier W.D., 2021. The Geotectonic Setting, Age and Mineral Deposit Inventory of Global Layered Intrusions. Earth-Science Reviews 220, 103736. https://doi.org/10.1016/j.earscirev.2021.103736.

Söderlund U., Johansson L., 2002. A Simple Way to Extract Baddeleyite (ZrO_2). Geochemistry, Geophysics, Geosystems 3 (2). https://doi.org/10.1029/2001GC000212.

Stacey J.S., Kramers J.D., 1975. Approximation of Terrestrial Lead Isotope Evolution by a Two-Stage Model. Earth and Planetary Science Letters 26 (2), 207–221. https://doi.org/10.1016/0012-821X(75)90088-6.

State Geological Map of the USSR, 1983. Scale 1:1000000. Sheet R-48-(50) (Olenek). VSEGEI Publishing House, Leningrad (in Russian) [Государственная геологическая карта СССР. Масштаб 1:1000000. Лист R-48-(50) (Оленёк). Л.: ВСЕГЕИ, 1983].